J Mater Sci (2007) 42:4935–4941
DOI 10.1007/s10853-006-0701-8

Mechanical interaction between single-walled carbon nanotubes during the formation of a bundle

Tania Vodenitcharova · Kausala Mylvaganam · Liang Chi Zhang

Received: 21 September 2005 / Accepted: 24 July 2006 / Published online: 9 March 2007

Abstract This paper investigates the intertubular van der Waals interactions that produce the initial cross sectional distortion of single-walled carbon nanotubes during a bundle formation. By combining the analysis of molecular dynamics with the continuum mechanics, the distributions of the van der Waals forces were determined. The dependence of the load parameters, deformation variables and the lattice constant on the nanotube radius, was also investigated. It was found that the van der Waals forces are attractive and vary circumferentially in a harmonic manner. For the considered zigzag nanotubes of radius 7–14 Å, the intensity of the van der Waals forces is radius-dependent and can be as large as 6–11 GPa in the channels of the bundle and 1–5 GPa at the closest points between the single-walled nanotubes.

Introduction

The outstanding properties of both single-walled nanotubes (SWNTs) and multi-walled nanotubes (MWNTs) make them the ideal building block for nanotechnology, nanoelectronics and nanomachines. They have been regarded as the strongest fillers in composite materials, owing to their high tensile strength and large failure strain. SWNTs have shown strong adhesion to each other, as a result of the strong van der Walls (vdW) interactions for radii in the range of a few nanometres. High-resolution transmission electron microscopy and electron diffraction studies indicated that the SWNTs are arranged in bundles with close-packed stacking, forming self-organized cables (e.g., [1]). Various techniques such as ultrasonication [2], high shear mixing [3], functionalization [4], viscous shearing [5], etc., have been used to disperse the nanotubes. In addition, Shen et al. [6] demonstrated that SWNT bundles could be split in situ with an atomic force microscope tip. These individual nanotubes have potential applications in new quantum electronic devices. On the other hand, novel devices based on nanotube bundles have also been reported [7]. Recently, Kang et al. [8] introduced a carbon nanotube oscillator based on SWNT bundles that can be operated by the excess vdW energy. Moreover, the strong cohesiveness provided by the vdW interactions between the SWNTs in a bundle can also be used for the manufacturing of larger fibres. Thus, a good understanding of the adhesion between SWNTs and their physical and mechanical properties in general, is of great importance.

In recent years the mechanical properties and behaviour of individual SWNTs and bundles have been extensively studied by molecular dynamics (MD) analysis. Despite their discrete molecular structures, SWNTs behave like continuum tubes and possess both membrane and bending capacities. This has allowed researcher to treat the nanotubes as a continuum, and to apply the well-established approaches of continuum/structural mechanics. A large number of studies have been conducted over the years to find the 'equivalent' geometric and material parameters that will map the nanostructural characteristics into macrostructural properties. The mechanics modelling though has been associated with various assumptions about the geometry of the nanotubes, as some treated them as space trusses, solid cylinders, or thin shells. The thin-shell assumption, (e.g., [9–11]) has also been an object of

T. Vodenitcharova · K. Mylvaganam · L. C. Zhang (✉)
School of Aerospace, Mechanical and Mechatronic Engineering, The University of Sydney, Sydney, NSW 2006, Australia
e-mail: zhang@aeromech.usyd.edu.au

intensive debate. Some researchers have adopted the interplanar spacing of graphite layers d_g = 3.42 Å to be the wall thickness h, and calculated the Young's modulus E as around 1 TPa with the axial stiffness estimated by MD. Others have used both axial and bending rigidities from experiments and MD, and concluded that h is smaller than the C–C bond length (e.g., h = 0.66 Å in Ref. [9]), and E is larger than 1 TPa (i.e., 5.5 TPa in Ref. [9]). Using the synchrotron X-ray diffraction results in Ref. [12], Vodenitcharova and Zhang [13] found that in the framework of continuum mechanics, h = 0.617 Å and E = 4.88 TPa for an SWNT with a radius of 7.04 Å; these parameters were subsequently used to adequately characterise the bending phenomenon of SWNTs [14]. The authors also predicted the deformation of a SWNT bundle subjected to external pressure of up to 1.5 GPa, which perfectly matches the experimental and MD results reported in Ref. [12].

The continuum theories of circular shells/rings usually assume a perfectly circular initial shape and no initial stressing, so the 'total' deformation is caused solely by external stresses. However, extensive MD simulations and experiments on SWNT bundles have shown that individual SWNTs in a bundle are deformed in an initial, externally unstressed state due to the intertubular van der Waals forces [15–17]. The SWNTs are flattened, the lattice constant ξ, as defined in Fig. 1, decreases and the distance between the SWNTs, called equilibrium distance d, becomes smaller than the equilibrium distance between two graphite layers of d_g = 3.42 Å. At a distance equal to d, the resultant forces of interaction between the neighbouring SWNTs are zero, at a distance larger than d the nanotubes attract each other; and at a distance smaller than d the intertubular interaction becomes repulsive. It has been found that the faceting of the SWNTs in a bundle is radius-dependent [15]—at small radii, the cross sections of SWNTs remain almost circular, but at large radii the cross-sectional distortion becomes noticeable. Thus, neglecting the initial faceting in the continuum mechanics modelling of large nanotubes, will underestimate the deformation under a specified pressure level, or will overestimate the pressure inducing specific deformation. While previous studies have reported the responses of carbon SWNT bundles subjected to external forces [18–20], there are no detailed reports on the interactions between the nanotubes in an unstressed state.

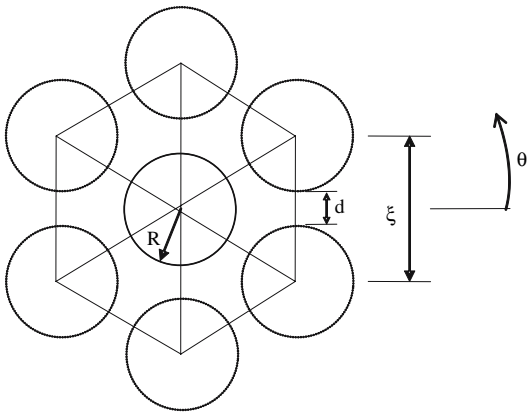

Fig. 1 Nanobundle geometry, where R is the radius of an undeformed SWNT, ξ is the lattice constant, d is the equilibrium distance between the SWNTs and θ is the circumferential coordinate

It is the aim of the present paper to clarify this issue, and to evaluate the distribution of the van der Waals forces that cause the bundle polygonization, as well as the influence of the nanotube radius. This fundamental knowledge will be useful to understand the function of novel devices based on nanotube bundles.

This study will combine MD simulations and continuum mechanics for the deformation of a number of zigzag-SWNT bundles of different radii. First the cross-sectional deformation of the nanotubes will be obtained by energy minimization using MD, and then the ring theory will be applied to reveal the mechanical interaction between the central nanotube and the surrounding nanotubes in the bundle, which would induce that deformation. The study will use h = 0.617 Å and E = 4.88 TPa, as estimated in Ref. [13] for a SWNT having R = 7.04 Å, since it has already been noted that both E and h are independent on helicity [21], and that the dependence of E on the radius is very weak for nanotubes of $R > 5$ Å [22].

Molecular dynamics simulation

Classical MD simulations were used to produce the deformation pattern of SWNT bundles in unstressed state. In the simulations, the inter-atomic forces were calculated using an analytical reactive empirical bond-order potential formulated by Brenner [23, 24], coupled to a long-range Lennard-Jones potential, i.e., $U(r) = 4\varepsilon[(\sigma/r)^{12} - (\sigma/r)^{6}]$ with parameters ε = 4.412 meV and σ = 3.35 Å [25]. This many-body potential has been extensively used to study the mechanical properties of carbon nanotubes [9, 26–28], and gave comparable predictions with ab initio calculations [29, 30]. Currently, many-body empirical potentials are the only way to model systems containing more than 1,000 atoms, to a reasonable accuracy. In this paper, open single-walled zigzag nanotubes were used to construct the nanotube bundle model. The energy of a SWNT was minimized using the conjugate gradient algorithm. A Berendsen thermostat was applied to all the atoms to minimize the heat conduction problem as pointed out in Ref. [27]. Then a bundle having seven of these SWNTs was constructed in a hexagonal arrangement as shown in Fig. 1; the surrounding six tubes were placed symmetrically with a gap of 3.1 Å.

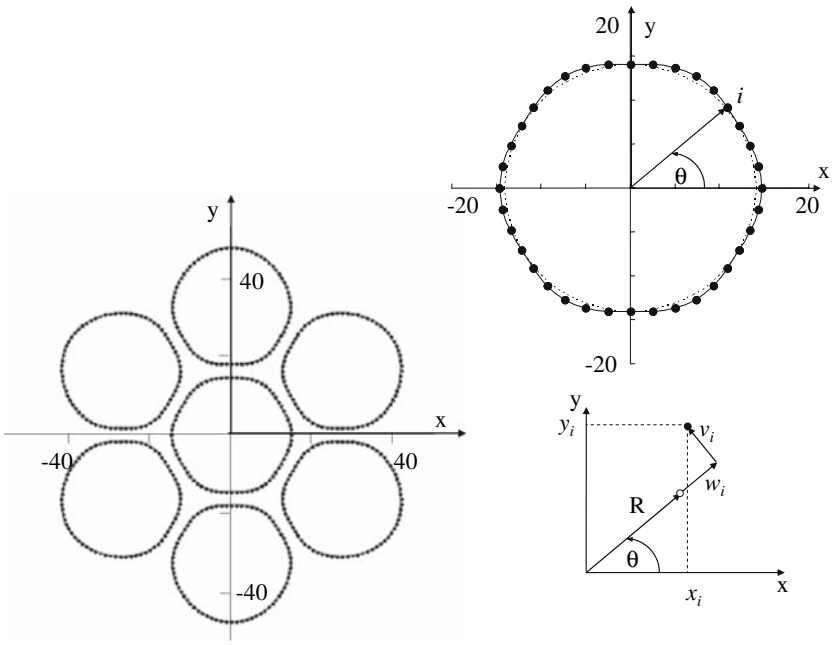

Fig. 2 Cross-sectional view of the deformed (36,0) SWNT bundle obtained by the MD simulation. The coordinate unit is Å. The top insert shows the cross section of the central nanotube: the dotted curve denotes the initial circular shape, the solid circles represent the locations of the atoms as obtained by the MD simulation, and the solid curve is the continuum mechanics prediction. The bottom insert shows an arbitrary atom *i* before deformation (hollow circle) and after deformation (solid circle), w_i and v_i are, respectively, the radial displacement (positive outward) and the tangential displacement (positive in the direction of positive θ); x_i and y_i are the coordinates of the *i*th atom after deformation

To understand the deformation characteristics of the SWNTs in a bundle, six different bundles, formed by (18,0), (20,0), (24,0), (28,0), (32,0) and (36,0) zigzag SWNTs, were investigated (the cross section of a (36,0) SWNT bundle is shown in Fig. 2). Then, the displacements of the atoms were used to calculate the distribution of the vdW interactions, which if applied along the circumference of the nanotube, would produce those displacements.

Continuum mechanics modelling

Let us consider the deformation of the central SWNT in a long bundle subjected to the van der Waals forces only. Using continuum mechanics, the nanotube can be presented as a thin cylindrical tube having a radius R and a wall thickness h, and the vdW forces can be replaced by a statically equivalent distributed load $p(\theta)$, varying along the circumference. According to the thin shell theory, it suffices to study the deformation of the mid-surface of the continuum nanotube, each point of which can undergo displacements in the longitudinal, circumferential and radial directions, i.e., u, v and w, measured from the undeformed geometry. Thus, zero displacements u, v and w will correspond to an isolated SWNT with no forces acting on it.

Since the length of a SWNT in a bundle is much greater than its diameter and the vdW forces along the SWNT axis can be considered uniform, the SWNT can be modelled as a ring of unit length under plane-strain deformation, and the longitudinal displacement u can be neglected. The only remaining displacements therefore are the radial displacement w (positive outward) and the tangential displacement v (positive in the direction of positive θ, Fig. 3). The discrete values of w and v at the atoms were provided by the

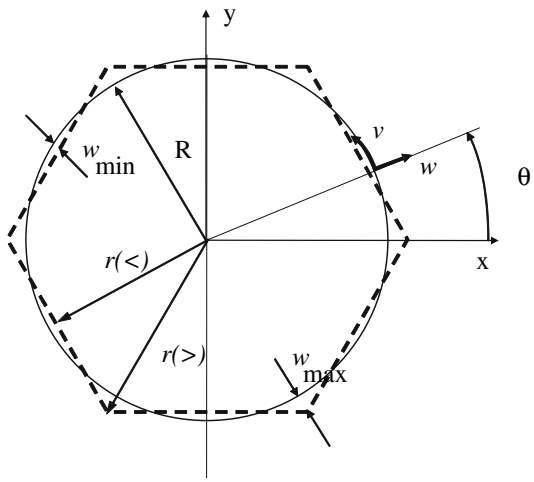

Fig. 3 The central SWNT in a bundle and the notations used in the continuum mechanics model. The solid line represents the initial undeformed shape, and the broken line symbolises the deformed configuration

MD simulations, so our aim was to determine the continuous functions $w(\theta)$ and $v(\theta)$ induced by $p(\theta)$. As the ring is in static equilibrium, $w(\theta)$, $v(\theta)$ and $p(\theta)$ have to minimise the potential energy of the ring $\Pi = U + W$; here U is the strain energy and W is the work done by the external load $p(\theta)$,

$$U = \frac{1}{2}EAR\int \varepsilon^2\,\mathrm{d}\theta + \frac{1}{2}EIR\int k^2\,\mathrm{d}\theta, \tag{1}$$

where $A = 1 \times h$ and $I = 1 \times h^3/12$ are, respectively, the cross-sectional area and the second moment of inertia of the ring cross-section; ε is the direct strain at the centroidal axis and k is the curvature change of the centroidal axis. The work done by $p(\theta)$ (assumed normal to the deformed surface) is associated only with w:

$$W = R\int_0^{2\pi} p(\theta)w\,\mathrm{d}\theta. \tag{2}$$

Further, ε and k can be expressed in terms of w and v as [31]:

$$\begin{aligned}\varepsilon &= \frac{v' + w}{R},\\ k &= \frac{(v - w')'}{R^2},\end{aligned} \tag{3}$$

where the prime means a derivation with respect to θ.

The displacement functions w and v, and the intensity of the vdW forces p (positive in compression) can be expressed by a Fourier series

$$\begin{aligned}w(\theta) &= \sum_0^\infty W_n\cos(n\theta),\\ v(\theta) &= \sum_0^\infty V_n\sin(n\theta),\end{aligned} \tag{4}$$

and

$$p(\theta) = \sum_0^\infty P_n\cos(n\theta), \tag{5}$$

where W_n, V_n and P_n are the weighting coefficients in the harmonic functions, which need to be determined. The first term in Eq. 5 (i.e., $n = 0$) represents a pressure (if positive) causing uniform contraction, or a tension (if negative) causing uniform expansion. The terms with $n = 1, 2, 3,...$ produce the faceting that has already been observed in experiments and MD simulations. By observation however, it is clear that the six SWNTs surrounding the central SWNT in the bundle are equally spaced and the bundle has six planes of symmetry at the interval of $\theta = 30°$ (i.e., $\theta = 0°, \pm30°, \pm60°$ and 90°). Thus $w(\theta)$ and $p(\theta)$ have the same symmetry (Fig. 4), and v vanishes there. As a result, the only non-zero terms in Eqs. 4 and 5 are those with $n = 0, 6, 12, 18,...$ for w and p, and $n = 6, 12, 18,...$ for v.

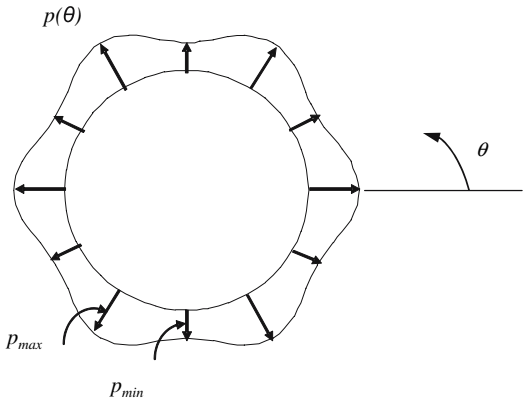

Fig. 4 Distribution of the van der Waals attraction on an SWNT as calculated from the continuum mechanics model

We need to determine W_n, V_n and P_n for the provided discrete values of w_i and v_i at all atoms. To do this, we have to write first the potential energy Π in terms of w, v and p, using formulae (1)–(5). Then the condition of minimising Π reads

$$\begin{aligned}&\frac{\partial\Pi}{\partial W_0} = 0\\ &\frac{\partial\Pi}{\partial W_n} = 0, \quad n = 6, 12, 18\ldots\\ &\frac{\partial\Pi}{\partial V_n} = 0, \quad n = 6, 12, 18\ldots\end{aligned} \tag{6}$$

Equation 6 is a set of simultaneous linear algebraic equations for W_n and V_n, which when solved leads to

$$\begin{aligned}W_0 &= -\frac{P_0R^2}{EA},\\ W_n &= -\frac{P_nR^4}{EI(n^2-1)^2}\left(1 + \frac{I}{AR^2}\right),\\ V_n &= \frac{P_nR^2}{EA(n^2-1)^2}\left(n - \frac{AR^2}{nI}\right) \quad \text{for } n = 6,\ 12,\ 18\ldots.\end{aligned} \tag{7}$$

Further simplification can be made in the expression for $p(\theta)$ in Eq. 5 if only two terms of w ($n = 0, 6$) and one term in v ($n = 6$) are taken as sufficient to represent the deformation: $\cos(6\theta)$ can be replaced in Eq. 5 by $[1 - 2\sin^2(3\theta)]$:

$$p(\theta) = p_c + p_0\sin^2(3\theta), \tag{8}$$

where $p_c = P_0 + P_6$ is the constant component of $p(\theta)$; and $p_0 = -2P_6$ is the varying component that induces the cross-sectional distortion.

Results and discussion

Six different bundles formed by (18,0), (20,0), (24,0), (28,0), (32,0) and (36,0) zigzag SWNTs were studied. The initial vdW interaction energy of the circular tubes in a bundle is very small (2–4 meV/atom). This is in agreement with the results reported by Lopez et al. [17]. The strain energy induced during flattening was calculated as the difference in the minimum total energy of the bundle and the total energy of the isolated undeformed nanotubes. It was found that the strain energy varies from 8.3 meV/atom for a nanotube with a radius of 7.05 Å, to 7.2 meV/atom for a nanotube with a radius of 14.1 Å. Obviously, the strain energy decreases with the increase in radius, which shows that more energy is required to deform nanotubes of smaller radii.

Energy minimization of each bundle by the MD analysis led to the faceting of the cross sections of all the nanotubes. As a result the distance, d between the nanotubes changed. A typical deformation pattern of a (36,0) SWNT bundle is shown in Fig. 2, where each dot represents a carbon atom on the cross section of the bundle. It is clear that the central SWNT has been deformed significantly into a symmetrical faceting shape. Thus the coordinates of the atoms before deformation, x_i and y_i, and after deformation, $x_{i,c}$ and $y_{i,c}$, are provided by MD, and can be used for the calculation of the displacements of the atoms, w_i and v_i (Fig. 2). Bearing in mind that the radius-vector of an arbitrary point after deformation is the sum of its initial radius-vector and its displacement vector $\mathbf{w} + \mathbf{v}$, the coordinates of an atom after deformation can be expressed as:

$$\begin{aligned} x_{i,c} &= R\cos(\theta) + w_i\cos(\theta) - v_i\sin(\theta) \\ y_{i,c} &= R\sin(\theta) + w_i\sin(\theta) + v_i\cos(\theta). \end{aligned} \tag{9}$$

Since $x_{i,c}$ and $y_{i,c}$ are known, Eq. 9 provides the unknown w_i and v_i at each atom

$$\begin{aligned} w_i(\theta) &= x_{i,c}\cos(\theta) + y_{i,c}\sin(\theta) - R \\ v_i(\theta) &= -x_{i,c}\sin(\theta) + y_{i,c}\cos(\theta). \end{aligned} \tag{10}$$

The MD results show that the circumferential displacements v_i are negligible compared with the radial displacements w_i. This indicates that during the bundle formation the nanotube atoms displace predominantly radially.

Now the problem of determining $w(\theta)$ and $v(\theta)$ is reduced to interpolation of those functions through their known values w_i and v_i. We performed such interpolation for all six bundles, as we varied the weighting coefficients W_n and V_n, and the number of harmonics n in Eq. 4, in order to produce the best fit to w_i and v_i. Figure 2 shows that $w(\theta)$ for a (36,0) nanotube perfectly matches the MD results.

With known $w(\theta)$, the degree of distortion/faceting of a SWNT cross section can be consequently evaluated in terms of two quantities [12, 18]: (1) a distortion ratio η, which is the ratio of the shortest radius $r^{(<)}$ to the longest radius $r^{(>)}$, Fig. 3, and (2) the lattice constant ξ, which is the centre-to-centre distance between two SWNTs in the bundle, Fig. 1. Those parameters can be calculated as

$$\begin{aligned} r^{(<)} &= R + w_{\min}, \\ r^{(>)} &= R + w_{\max}, \\ \eta &= \frac{r^{(<)}}{r^{(>)}}, \\ \xi &= 2r^{(<)} + d \end{aligned} \tag{11}$$

where $w_{\min}$ is the minimum displacement (at the shortest distance between two adjacent nanotubes), and $w_{\max}$ is the maximum displacement at the points of SWNTs in the channels (i.e. the space formed by three adjacent SWNTs in the bundle).

The deformation of all six nanobundles was analysed using the constitutive model presented in section ''Continuum mechanics modelling'', and Eqs. 10 and 11 above, and the dependence of all quantities of interest on the nanotube radius R was examined. It appears that the lattice constant $\xi = 2r^{(<)} + d$ increases linearly when R increases (Fig. 5a), since d and w are small compared to R. Also, the intertubular distance d steadily increases from 3.19 Å to 3.34 Å for the range of radii considered, Fig. 5b. This result confirms the validity of the analysis because for a very large radius ($R \rightarrow \infty$), two neighbouring nanotubes will become equivalent to two flat graphite sheets, and hence d must approach $d_g = 3.42$ Å. The smallest and the largest radii, $r^{(<)}$ and $r^{(>)}$ of the central SWNT are also scaled linearly with R, Fig. 5c. However, the distortion parameter η decreases from 0.983 to 0.958 (Fig. 5d), which suggests that the non-uniform deformation in the circumferential direction becomes more pronounced for larger SWNTs.

It was found that only two terms in $w(\theta)$, i.e., W_0 and W_6, are sufficient to fit the maximum and minimum displacements $w_{\max}$ and $w_{\min}$; however, the third term W_{12} (although small) is also needed to accurately represent the displacements of other atoms. Both W_0 and W_6 appear to be positive Fig. 5e. For radii smaller than 11 Å, W_0 is greater than W_6, indicating an overall expansion of the nanotube,

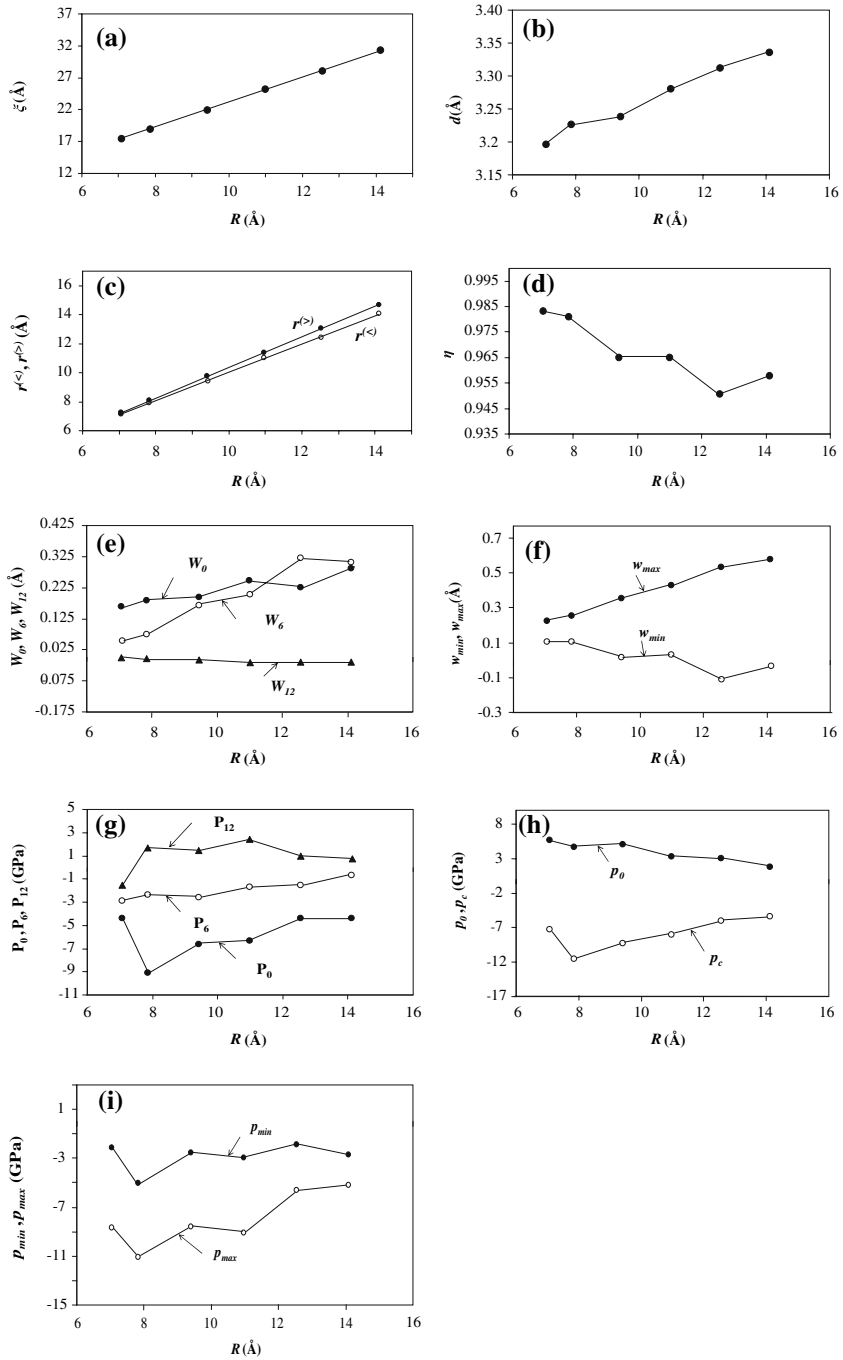

Fig. 5 Deformation and forces on central SWNTs in bundles. (**a**) Lattice constant ξ versus external radius, where the solid circles are the continuum mechanics fit to the MD results. (**b**) Shortest distance d between the SWNTs in a bundle versus radius, where the solid circles are the MD results. (**c**) Shortest and longest radii $r^{(<)}$ and $r^{(>)}$ of the deformed SWNT cross section versus radius, where the circles are the continuum mechanics fit to the MD results. (**d**) Distortion ratio η versus radius, where the solid circles are the continuum mechanics fit to the MD results. (**e**) Terms in the Fourier expansion of $w(\theta)$ versus radius, where the circles and triangles are the continuum mechanics fit to the MD results. (**f**) Maximum (in the channels) and minimum (at the closest points between the nanotubes) radial displacement w, where the circles are the continuum mechanics fit to the MD results. (**g**) Terms in the Fourier expansion of the van der Waals force $p(\theta)$ versus radius, where the circles and triangles are the continuum mechanics fit to the MD results. (**h**) Terms in the Fourier expansion of $p(\theta)$ versus radius if only two terms in Eq. 1 are considered, where the circles are the continuum mechanics fit to the MD results. (**i**) Maximum (in the channels) and minimum (between the SWNTs) $p(\theta)$ versus radius, where the circles are the continuum mechanics fit to the MD results. Note that $p(\theta)$ is positive in compression

in spite of the flattening effect. In other words, the radial displacement in this case is outward ($w_{min} > 0$) even at the shortest distance between the SWNTs, Fig. 5f. For radii greater than 11 Å, W_6 becomes slightly greater than W_0 and w_{min} turns out to be negative. In this case, the non-uniform inward displacement dominates at the points of minimum intertubular distance.

Of particular importance is the determination of the vdW interactions $p(\theta)$. The loading parameters P_n in Eq. 5 are now easy to calculate using Eq. 7, as W_n and V_n are already known. The values of P_n are radius-dependent, Fig. 5g, as only the first three harmonics ($n = 0$, 6, 12) are more significant while the others are negligible. P_{12} has a small contribution though, and if it is neglected, the vdW interactions $p(\theta)$ can be presented by two terms in the form of Eq. 8, where p_c is a constant term, and $p_0 \sin^2(3\theta)$ is a positive-definite term varying along the circumference and producing the faceting effect. Both p_0 and p_c decrease when the nanotube radius increases, Fig. 5h. This suggests that the bundle formation of larger nanotubes is associated with smaller vdW forces. It appears that $p(\theta)$ is attractive (negative sign means attraction) and attains its maximum value p_{max} in the channels, where the attraction between the neighbouring atoms of the adjacent nanotubes is more significant. The minimum value p_{min} appears at the points of minimum intertubular distance, where the attraction between the neighbouring atoms is small. Nevertheless, both p_{min} and p_{max}, are significant, Fig. 5i. For the considered nanotube radii, p_{max} vary from 6 GPa to 11 GPa and p_{min} from 1 GPa to 5 GPa.

Conclusions

Subjected to the van der Waals adhesion, carbon SWNT bundles deform during formation and reach mechanical stability. By applying a continuum mechanics approach to the deformation provided by molecular dynamics, we predicted the adhesive properties of zigzag SWNT bundles, and their variation with the nanotube radius. We can conclude that the neighbouring nanotubes in a bundle attract each other, with the maximum attraction of 6–11 GPa in the channels, and minimum attraction of 1–5 GPa at the shortest distance between the SWNTs. The radius of SWNTs plays an important role in the deformation of the nanobundle. In larger nanobundles the cross-sectional distortion and the distance between the SWNTs is more pronounced. An SWNT with radius smaller than 11 Å will experience an overall expansion in a bundle.

Acknowledgement This research was supported by an ARC Discovery Grant.

References

1. Zhang Y, Ichihashi T, Landree E, Niley F, Iijima S (1999) Science 285:1719
2. Schadler LS, Giannaris SC, Ajayan PM (1998) Appl Phys Lett 73(26):3842
3. Geng H, Rose R, Zheng B, Shimoda H, Fleming L, Liu J, Zhou O (2002) Adv Mater 14:1387
4. Viswanathan G, Chakrapati N, Yang H, Wei B, Chung H, Cho K, Ryu CY, Ajayan PM (2003) J Am Chem Soc 125:9258
5. Xiao K, Zhang LC (2005) J Mat Sci 40:6513
6. Shen Z, Liu S, Hou S, Gu A, Xue Z (2003) J Phys D: Appl Phys 36:2050
7. Bockrath M, Cobden DH, Mceuen PL, Chopra NG, Zettl A, Thess A, Smalley RE (1997) Science 275:1922
8. Kang JW, Song KO, Hwang HJ, Jiang Q (2006) Nanotechnology 17:2250
9. Yakobson BI, Brabec CJ, Bernholc J (1996) Phys Rev Lett 76(14):2511
10. Ru CQ (2002) Phys Rev B 62(15):9973
11. Pantano A, Parks D, Boyce M (2004) J Mech Phys Solids 52:789
12. Tang J, Qin L-C, Sasaki T, Yudasaka M, Matsushita A, Iijima S (2000) Phys Rev Lett 85(9):1887
13. Vodenitcharova T, Zhang LC (2003) Phys Rev B 68:16540
14. Mylvaganam K, Vodenitcharova T, Zhang LC (2006) J Mater Sci 41:3341
15. Tersoff J, Ruoff RS (1994) Phys Rev Lett 73(5):676
16. Charlier J-C, Lambin P, Ebbesen TW (1996) Phys Rev B 54(12):R8377
17. Lopez MJ, Rubio A, Alonso JA, Qin L-C, Iijima S (2001) Phys Rev Lett 86(14):3056
18. Venkateswaran UD, Rao AM, Richter E, Menon M, Rinzler A, Smalley RE, Eklund PC (1999) Phys Rev B 59(16):10 928
19. Ni B, Sinnot S (2001) Surf Sci 487:87
20. Elliott JA, Sandler JKW, Windle AH, Young RJ, Shaffer MSP (2004) Phys Rev Lett 92:095501
21. Xin Z, Jianjun Z, Zhong-Can O-Y (2000) Phys Rev B 62(20):13692
22. Li C, Chou T-W (2003) Int J Solids Struct 40(10):2487
23. Brenner DW (1990) Phys Rev B 42:9458
24. Brenner DW, Shenderova O, Harrison J, Stuart S, Ni B, Sinnot TS (2002) J Phys: Condensed Matter 14:783
25. Allen MP, Tildesley DJ (1987) Computer simulation of liquids. Clarendon Press, Oxford
26. Garg A, Han J, Sinnot S (1998) Phys Rev Lett 81:2260
27. Mylvaganam K, Zhang LC (2004) Carbon 42:2025
28. Mylvaganam K, Zhang LC (2006) Nanotechnology 17:410
29. Claire PDS, Son K, Hase WL, Brenner D (1996) J Phys Chem 100:1761
30. Mylvaganam K, Zhang LC (2006) Key Eng Mat 312:217
31. Farshad M (1994) Stability of structures. Elsevier Science, Amsterdam